Eur. Phys. J. B **53**, 439–448 (2006)
DOI: 10.1140/epjb/e2006-00406-4

THE EUROPEAN PHYSICAL JOURNAL B

Synthesis and optical properties for crystals of a novel organic semiconductor $[Ni(Cl)_2\{(Ph_2P)_2CHC(R_1R_2)NHNH_2\}]$

A.M. Badr[1,a], A.A. EL-Amin[1], and A.F. Al-Hossainy[2]

[1] Physics Department, Faculty of Science, South Valley University, Aswan, Egypt
[2] Chemistry Department, Faculty of Science, South Valley University, Aswan, Egypt

Received 17 June 2006 / Received in final form 5 August 2006
Published online 17 November 2006 –

Abstract. In this investigation, the synthesis process of the apyrazole derivative for diphenylphosphino-methane hydrazine complexes $[Ni(Cl)_2\{(Ph_2P)_2CHC(R_1R_2)NHNH_2\}]$ was reported, and the obtained crystals were analyzed by X-ray diffraction. As a result of the growth process, a set of complexes were formed. The structures of these complexes are discussed on the basis of Elemental analysis (EA), IR, ^{1}H-NMR, ^{31}P-NMR spectroscopic data and FAB mass spectra. The compound under investigation shows typical semiconductor behavior as a result of delocalization of the π-electrons in the structure. The reflectance and transmittance spectra for the crystals were measured and analyzed in the incident photon energy range 1.29 to 3.93 eV and in the temperature range 77 to 300 K. The optical study revealed that the optical transition is direct allowed. Below the absorption edge, the refractive index as a function of wavelength was determined in the low energy region of the used incident photon energy range. From the refractive index-wavelength variations, the oscillator and dispersion energies of the refractive index for the obtained crystals were determined. The static refractive index and static dielectric constant were evaluated.

PACS. 31.10.+z Theory of electronic structure, electronic transitions, and chemical binding – 31.70.-f Effects of atomic and molecular interactions on electronic structure – 74.25.Gz Optical properties – 78.20.-e Optical properties of bulk materials and thin films

1 Introduction

Organic semi-conducting materials can be grouped as either polymers, monomers, or organic compounds. The current revival of interest in the electronic properties is reflected by a considerable increase in the number of investigations dealing with the measurement of electrical conductivity. These materials are of great interest in electronic devices and have a number of advantages because of the variety of structures. The importance of their electrical transport properties were led to different aspects of the conduction mechanism, nature of charge carriers and their properties being studied [1]. Organic semiconductors show great promise for applications in electronics, photonics, xerography, thin film transistors, light emitting diodes, solar cells and many others [2–4]. However, the nature of charge transport and primary photo-excitations in conjugated organic molecular crystals is not completely understood [5].

The study of organic semiconductors continues to generate interest with the reports of completely new materials possessing novel features. Many inclusion and charge transfer organic complexes were studied both experimentally and theoretically under different conditions such as temperature and pressure. It is already known that the organic semiconductors can also be treated as the conventional semiconductors but with partially stabilized conduction bands [6]. In semiconductors, the absorption coefficient falls exponentially near the optical absorption edge [7]. The tail states can be either within the conduction or valence band or extending within the forbidden energy gap. This so called Urbach tail is of the order of the thermal energy for ordered materials [8]. Band tailing reduces the band gap or the activation energy and increases conductivity. Our attention has been centered on the substitution reaction involving the loss of carbon monoxide from hexanuclear metal carbonyl compounds $[M(NI)_6]$ induced by the bidentate phosphine ligand $[(Ph_2P)_2CH_2]$. In last two decades there has been a great deal of interest in the preparation and properties of

[a] e-mail: badr_egsc@yahoo.com

transition metal carbonyl complexes stabilized with multidentate ligands [9–15].

The optical and electrical properties of the metal complexes are of increasing interest in the area of semiconducting and optical materials because these materials possess great potential for device applications such as Schottky diodes, solid state devices and optical sensors. So, it is important to investigate the optical properties of all new optical materials based on metal complexes. In this study, we report the preparation of cationic Nickel (II) complexes containing $Ph_2PCH_2PPh_2$[dppm = bis(diphenylphosphinyl)methane] of the type [Nidppm](Cl)$_2$. The crystals obtained have a transparent appearance. The temperature dependence of their optical properties and parameters have been characterized and are discussed based on the analyses of the optical measurements under the temperature range 77 to 300 K.

2 Experimental set-up

2.1 Preparation of organometallic compounds

(i) [$NiCl_2$. $6H_2O$] (0.1 g, 0.42 mmol), {$(Ph_2P)_2CH_2$}] (0.161 g, 0.42 mmol), n-decane (25 cm^3) were placed in a 500 cm^3 heavy-walled glass pressure vessel. The mixture was saturated with N_2. The reaction vessel was heated to 70 °C for 40 min, with string, and then cooled, and the solution filtrate was reduced in volume. The solution filtrates were treated under vacuum vessel and washed using a petroleum ether-ethanol of 5:1. The precipitates were collected; a pale red precipitate of [Cl_2Ni{$(Ph_2P)_2CH_2$}]. A pale yellow precipitate was recrystallized from ether-methanol to give yellow crystals of [Cl_2Ni{$(Ph_2P)_2CH_2$}] (compound: 1a in the scheme). Yield (0.196 g, 91.16%), found: C, 58.69; H, 4.19; Cl, 14.03%. Calc.: C, 58.42; H, 4.31; Cl, 13.80%. $m/z = 511.99$ (mass spectrometry; Tab. 1).

(ii) Phenylacetone in toluene [CH_3CoPh] (0.5 cm^3), was added to a suspension of [Cl_2Ni{$(Ph_2P)_2CH_2$}] (0.149 g, 0.29 mmol). The mixture was then heated to *ca.* 80 °C for 1 h. During which the Nickel complex dissolved and a new pale brown crystalline precipitate formed. This was filtered off, washed with Et_2O and dried giving the required product [Cl_2Ni{$(Ph_2P)_2C{=}CCH_3(Ph)$}] Yield (0.15g, 83.80%). The pale brown precipitate [Cl_2Ni{$(Ph_2P)_2C{=}CCH_3(Ph)$}] was recrystallised from ether-methanol to give pale brown crystals (compound: 2a in the scheme): C, 65; H, 4.53; Cl, 11.63%. Calc.: C, 64.33; H, 4.58; Cl, 11.51%. $m/z = 614.27$ (mass spectrometry; Tab. 1).

(iii) Hydrazine hydrate [NH_2NH_2] (0.5 cm^3), was added to a suspension of [Cl_2Ni{$(Ph_2P)_2C{=}CCH_3(Ph)$}] (0.197 g, 0.32 mmol) in toluene. The mixture was then heated to *ca.* 80 °C for 15 min. During which the Nickel complex dissolved and a brown crystalline precipitate formed. This was filtered off, washed with Et_2O and dried giving the required product [Cl_2Ni{$(Ph_2P)_2CHC(NHNH_2)CH_3(Ph)$}] Yield (0.147 g, 71.01%). The brown precipitate [Cl_2Ni{$(Ph_2P)_2CHC(NHNH_2)CH_3(Ph)$}] was recrystallized from ether-methanol to give brown crystals (compound: 3a in the scheme): C, 61.33; H, 5.03; Cl, 10.90; N, 4.41%. Calc.: C, 61.15; H, 4.98; Cl, 10.94; N, 4.32%. $m/z = 648.12$ (mass spectrometry; Tab. 1).

(iv) [Cl_2Ni{$(Ph_2P)_2CHC(NHNH_2)CH_3(Ph)$}] (0.156 g, 0.24 mmol) in toluene (1 cm^3) and acetylacetone $CH_3NICH{=}C(OH)CH_3$ (0.25 cm^3) was heated under reflux for 16 h to give apyrazole. The resulting yellow solution was evaporated to low volume under reduced pressure and ethanol added. The product separated [Cl_2Ni{$(Ph_2P)_2CHC(NHN{=}C(CH_3)CH{=}$ $C(OH)CH_3)CH_3(Ph)$}] as yellow prisms (compound: 4a in the scheme). Yield 0.161g (91.48%), found: C, 62.87; H, 5.35; Cl, 9.63; N, 3.74%. Calc.: C, 62.5; H, 5.24; Cl, 9.71; N, 3.84%. $m/z = 728$ (mass spectrometry; Tab. 1). **(v)** [Cl_2Ni{$(Ph_2P)_2CHC(NHN{=}C(CH_3)CH{=}$ $C(OH)CH_3)CH_3(Ph)$}] in toluene (1 cm^3) was heated under reflux for 16 h. The resulting pale blue solution was evaporated to low volume under reduced pressure and ethanol added to obtain the apyrazole derivative with acetylacetone. The [Cl_2Ni{$(Ph_2P)_2CHC(N^*N{=}C(CH_3)$ $CH{=}C^*CH_3)CH_3(Ph)$}] product is thereafter separated (compound: 5a in the scheme). Yield 0.165 g (85.93%), found: C, 64.23; H, 5.00; Cl, 10.14; N, 3.85%. Calc.: C, 64.08; H, 5.09; Cl, 9.96; N, 3.93%. $m/z = 710.11$ (mass spectrometry; Tab. 1).

2.2 Apparatus and techniques

The bulk sample used in optical measurements was prepared by splitting a suitable plate of the obtained crystals, and therefore the resulting surface was mirror-like without any mechanical treatment. Then it was mounted on the cold finger inside a cryostat (Oxford DN1704-type), which was evacuated to about 10^{-5} Torr. The temperature inside the cryostat was controlled by a digital temperature controller (Oxford ITC601-type). A UV-visible double beam spectrophotometer (model UV-1650PC) was employed to record the reflectance and transmittance spectra of the incident photon energy over the wavelength range from 315 to 960 nm. The the thickness of the cleaved sample used to record the mentioned spectra, was measured to be about 0.1 cm.

The melting points were recorded on a Galenkanp melting point apparatus. Elemental analyses were carried out at the Micro Analytical center (Assiut University). The IR spectra (KBr) were determined on a Shimadzu corporation Chart 200-91527 spectrophotometer. ^{1}H-NMR spectra were recorded with a Bruker AMX-250 spectrometer. Mass spectra were recorded on HpMs 6988 spectrometer and electron-impact (EI). The X-ray data were collected with a radiation of "$\lambda = 1.541838$ Å" (see Fig. 1).

Table 1. Characterization data of the newly synthesized (diphenylphosphino)methane derivative complexes.

Mol. formula (mol. wt.), No [Yield %]	Calcd.%,(Found) % C	H	Cl	N	m.p. °C	Coupling constants (Hz) $^2J(PCH_2)$ Hz	$^4J(PCH_3)$ Hz	$^2J(PCH)$ Hz	$^1H\{^{31}P\}$-NMR($C_2H_2Cl_4$/$(CD_3)_2CO$) δ, p.p.m., Assignment	M^+
$C_{25}H_{22}Cl_2NiP_2$ (513.99), 1a [91.16]	58.42 (58.69)	4.31 (4.19)	13.80 (14.03)	– –	250–252	11	–	–	2.09 (m, 2H, CH_2 methylene) [6.95(s, 4H, p-CH)], [7.11(s, 8H, o-CH)], [7.57(s, 8H, m-CH)] aromatic ring	511.99
$C_{33}H_{28}Cl_2NiP_2$ (616.12), 2a [83.80]	64.33 (65.00)	4.58 (4.53)	11.51 (11.63)	–	224–228	–	4	–	1.73 (s, 3H, CH_3 methyl) [6.82(s, 4H, p-CH)], [7.01(s, 8H, o-CH)], {7.57(s, 8H, m-CH)] aromatic ring	614.27
$C_{33}H_{32}Cl_2N_2NiP_2$ (648.17), 3a [71.01]	61.15 (61.33)	4.98 (5.03)	10.94 (10.90)	4.32 (4.41)	209–213	–	–	12	2.48 (wb, 1NH, $2NH_2$, amine) 6.47 (w, 1H, methine, 1 beta -N) 1.56 (s, 3H, methyl -CH) [6.85-7.57(s, 4H, 8H, 8H)] aromatic ring	682.05
$C_{38}H_{38}Cl_2N_2NiOP_2$ (730.27), 4a [91.48]	62.50 (62.87)	5.24 (5.35)	9.71 (9.63)	3.84 (3.74)	201–211	–	–	13	1.31 (s, 3H, methyl,1beta -N) 6.304 (w, 1H,methine, 1beta -N) 4.93 (m, 1H, 1-ethylene, 1alpha -C=C) 8.11(w, 1$\tilde{N}$H, hydrazid) 11.86 (w, enol (C-OH)) 1.82 (s, 3H, methyl, 1alpha –C=CH) 0.97 (s, 3H, methyl, 1gama C=CH-) [6.80–7.57 (m, 5H, 10H, 10H)] aromatic ring	728
$C_{38}H_{36}Cl_2N_2NiP_2$ (712.25), 5a [85.93]	64.08 (64.23)	5.09 (5.00)	9.96 (10.14)	3.93 (3.85)	198–203	–	–	12	6.494 (w, 1H,methine, 1beta -N) 5.89 (s, 1H, 1-pyrazole, 1alpha -N-) N=C-C1 2.52 (s, 3H, methyl, 1beta -N) 1.35 (s, 3H, methyl, 1 alpha -N-N=C-1) 2.13 (s, 3H, methyl, 1 alpha -N-N=C-CH=C-1) [6.80–7.55 (m, 4H, 8H, 8H)] aromatic ring	710.11

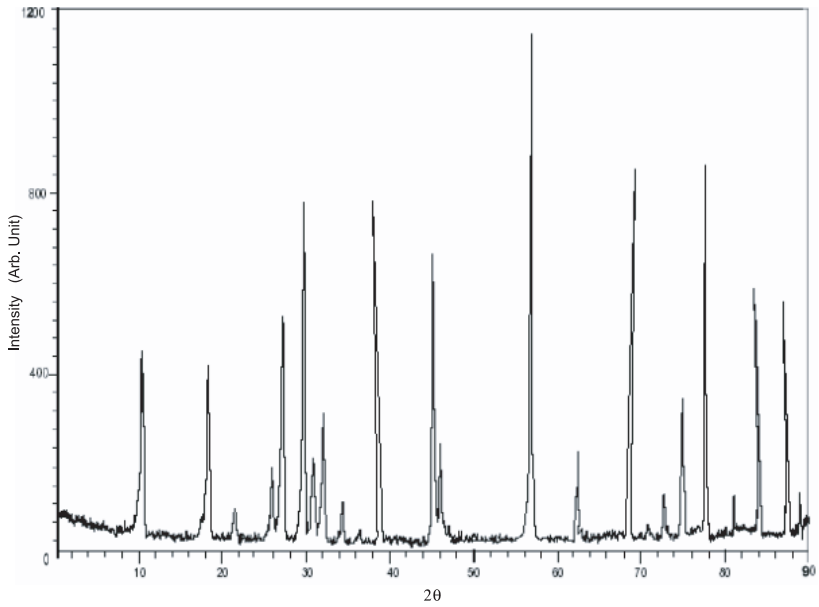

Fig. 1. X-ray diffraction pattern of the organic crystals under study "5a".

Table 2. ^{31}P-{^{1}H} n.m.r. data[a], and Infrared[b] data for some condensation and Michael additions products of [$(Cl)_2Ni\{(Ph_2P)_2CH_2\}$]: a) Chemical shifts, δ, to high frequency of 85% H_3PO_4; b) far infrared in KBr discs; c) υ(OH) = 3240 cm^{-1}.

Complex	$\delta(P)$p.p.m.	(ν Ni-Cl) and (υ P-C)/cm^{-1}	υ(NH)/cm^{-1}
1a	41.30	314 s, 290 s single band (ν Ni-Cl) 720 s, 690 s single band (ν P-C)	–
2a	47.90	315 s, 285 s single band (ν Ni-Cl) 710 s, 695 s single band (ν P-C)	–
3a	45.70	320 s, 290 s single band (ν Ni-Cl) 715 s, 680 s single band (ν P-C)	3300
4a[c]	43.90	314 s, 285 s single band (ν Ni-Cl) 710 s, 685 s single band (ν P-C)	3310
5a	40.80	310 s, 295 s single band (ν Ni-Cl) 725 s, 685 s single band (ν P-C)	–

3 Results and discussion

3.1 Characterization and structural properties

In this section, the synthesis and the characterization of the diphenylphosphino methane complexes and their derivatives are illustrated (see the scheme, Fig. 2, Tabs. 1 and 2):

(i) Treatment of Complex the [Nidppm]$(Cl)_2$ adduct: treatment of the [Nidppm]$(Cl)_2$ adduct in n-decane with a slight excess (20%) of phenylacetone gave [$(Cl)_2Ni\{(Ph_2P)_2C{=}CMe(Ph)\}$] after heating *ca* 1 h under dinitrogen, pale brown crystals of the Nickel complex adduct with a >80% yield. We assigned the structure of this adduct on the basis of (a) satisfactory elemental analysis (see experimental); (b) the ^{31}P-{^{1}H} n.m.r spectrum showed a singlet at δ = 47.90 p.p.m. with Ni satellites, ^{1}J(NiP)/Hz = zero; (c) the ^{1}H and ^{1}H-{^{31}P} n.m.r spectra showing four signals. At δ = 1.73 p.p.m. a strong singlet of relative intensity 3H is observed and assigned to CH_3, ^{4}J(P-C=C-CH_3) = 3 Hz. (Aromatic hydrogen) A triplet is centered at δ = 7.01 p.p.m, of relative intensity (s, 4H, p-CH), (s, 8H, o-CH) and (s, 8H, m-CH).

(ii) Addition of hydrazine hydrate: treatment of the [$(Cl)_2Ni\{(Ph_2P)_2C{=}CMe(Ph)\}$] adduct in toluene with a slight excess of Hydrazine hydrate gave [$(Cl)_2Ni\{(Ph_2P)_2CHCNH\text{-}NH_2Me(Ph)\}$] after heating *ca* 15 min under dinitrogen, brown crystals of the nickel hydrazine adduct with a >70% yield. We assigned the structure of this adduct on the basis of (a) satisfactory elemental analysis (see Tab. 1); (b) The ^{31}P-{^{1}H} n.m.r spectrum showed a singlet at δ = 45.70 p.p.m. with Ni satellites, ^{1}J(NiP)/Hz = zero; (c) the ^{1}H and ^{1}H-{^{31}P} n.m.r spectra showing three signals (excluding aromatic hydrogen). At δ = 1.56 p.p.m. a strong single of relative intensity 3H is observed and assigned to CH_3. At δ = 6.47 p.p.m. a triplet of relative intensity 1H is observed and assigned to CH, ^{4}J(C<u>H</u>-C-C<u>H</u>$_3$) = 2.1 Hz. Finally a broad signal is observed at δ = 2.48 p.p.m. of relative intensity 1H, assigned to the NH-NH_2 proton. This signal is due to NH disappearing on addition of D_2O. In the ^{1}H n.m.r spectrum, the coupling to phosphorus is shown by the protons CH^1, ^{2}J(<u>P</u>C<u>H</u>^{1}) = 12 Hz, and by CH_3 protons, ^{4}J(<u>P</u>-C=C-C<u>H</u>$_3$) = 2.7 Hz; (d) the infrared spectrum showing at υ(NH) at 3300 cm^{-1}.

(iii) Condensation with acetylacetone: treatment of the [$(Cl)_2Ni\{(Ph_2P)_2CHCNH\text{-}NH_2Me(Ph)\}$] adduct in toluene with a slight excess (20%) of acetylacetone gave [$Cl_2Ni\{(Ph_2P)_2CHC(NHN{=}C(CH_3)CH{=}C(OH)CH_3)CH_3(Ph)\}$] after heating for <u>*ca*</u> 1 h under dinitrogen, pale yellow crystals of the Nickel complex adduct with a >90% yield. We assigned the structure of this adduct on the basis of (a) satisfactory elemental analysis (see Tab. 1); (b) The ^{31}P-{^{1}H} n.m.r spectrum showed a singlet at δ = 43.90 p.p.m. with Ni satellites, ^{1}J(NiP)/Hz = zero; (c) the ^{1}H and ^{1}H-{^{31}P} n.m.r spectra showed seven signals (excluding aromatic hydrogen). At δ = 6.30 p.p.m. a triplet of relative intensity 1H is observed and assigned to CH, ^{4}J(C<u>H</u>-C-C<u>H</u>$_3$) = 2.3 Hz. A strong signal is centered at δ = 1.31 p.p.m. of relative intensity 3H, assigned to (-CH-C-CH_3) protons. A singlet at δ = 1.82 p.p.m of relative intensity 3H is observed, assigned to the (CH=C-CH_3) proton. A singlet at δ = 0.97 p.p.m. of relative intensity 3H is observed, assigned to (C=CH-CH_3) proton, A singlet at δ = 4.93 p.p.m. of relative intensity 1H is observed, assigned to ethylene –C=CH proton, a broad signal is observed at δ = 8.11 p.p.m. of relative intensity 1H, assigned to the NH proton. This signal due to NH disappeared on addition of D_2O. Finally a broad signal is observed at δ = 11.86 p.p.m. of relative intensity 1H, assigned to the OH proton. The signal due to OH disappeared on addition of D_2O. In the ^{1}H n.m.r spectrum the coupling to phosphorus is shown by the protons CH, ^{2}J(<u>P</u>C<u>H</u>^{1}) = 13 Hz; (d) the infrared spectrum showed υ(NH) at 3300 cm^{-1} and showed υ(OH) at 3240 cm^{-1}.

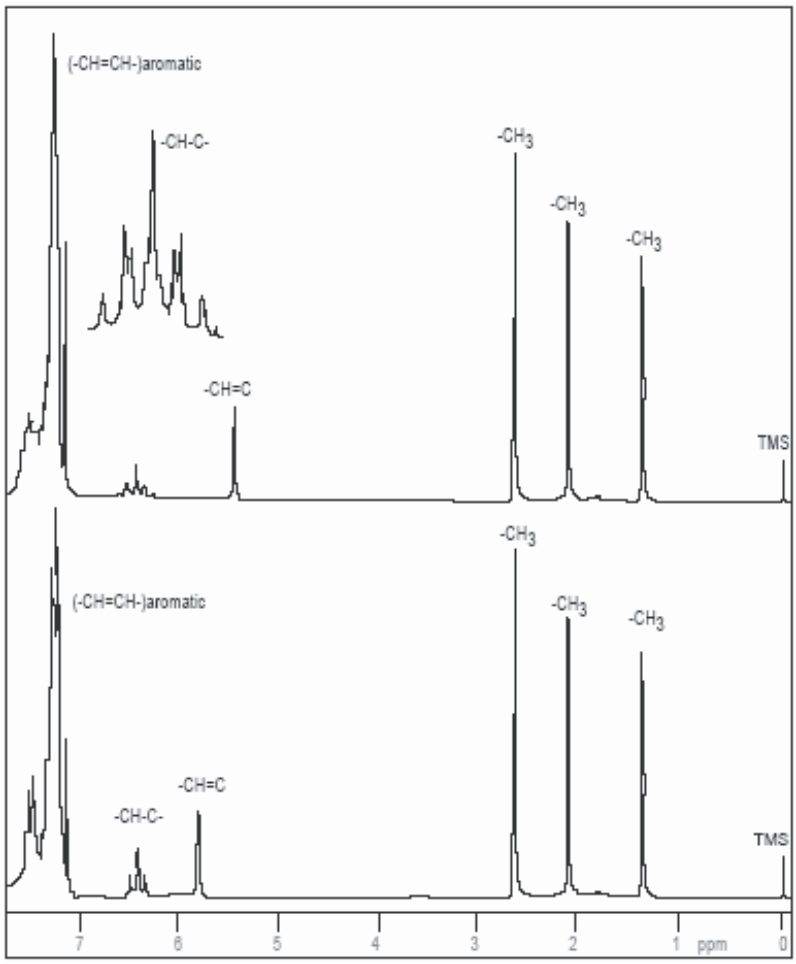

Fig. 2. ^{1}H-{^{31}P} and ^{1}H n.m.r spectra for the organic crystals under study "5a".

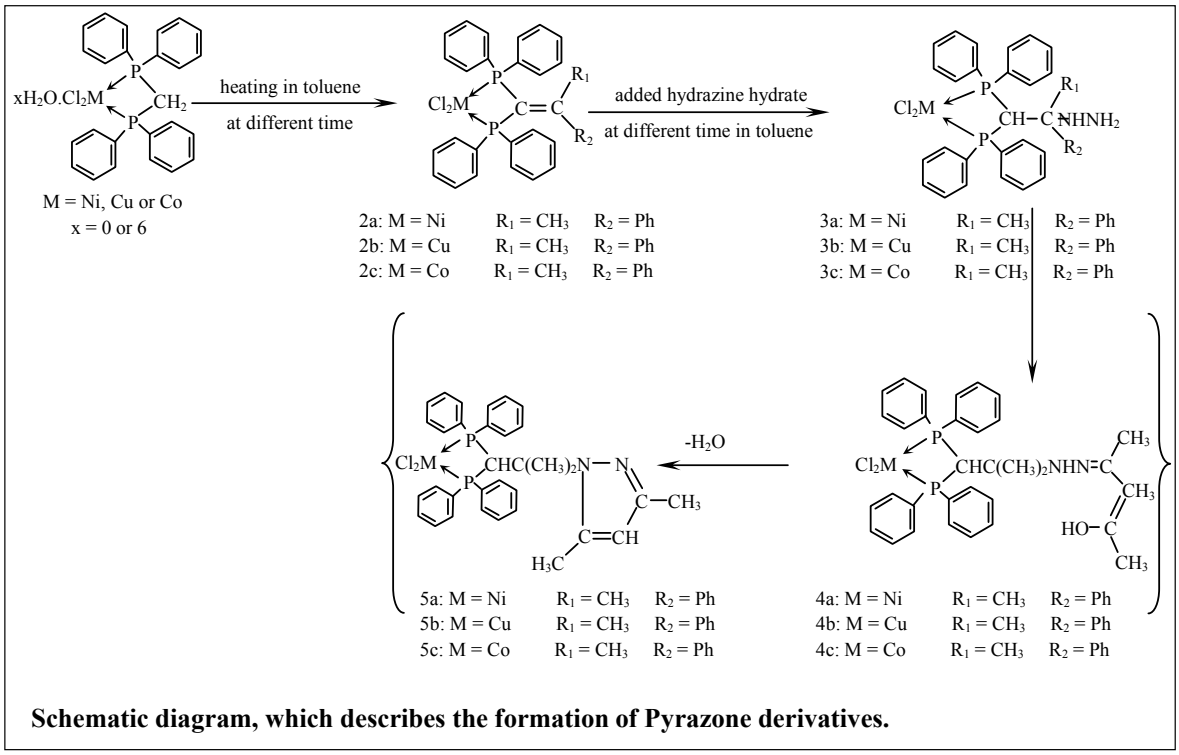

Schematic diagram, which describes the formation of Pyrazone derivatives.

(iv) Formation of a pyrazole derivative: Hydrazine complexes of the type $[(Cl)_2Ni\{(Ph_2P)_2CHCNH\text{-}NH_2Me(Ph)\}]$ were reacted with acetylacetone to give a pyrazole. On heating the nickel- hydrazine adduct with one mole equivalent of acetylacetone in toluene for a prolonged period (*ca.* 16 h), a pale blue crystalline product formed, which we formulated as the pyrazole derivative (5a). This complex was formulated on the following basis: (a) the $^{31}P\text{-}\{^1H\}$ n.m.r spectrum showed a singlet at $\delta = 40.80$ p.p.m. with Ni satellites. $^1J(NiP)/Hz$ = zero (see Tab. 2) for data; (b) the $^1H\text{-}\{^{31}P\}$ and ^1H n.m.r spectra, (see Fig.2) showed five signals. At $\delta = 6.49$ p.p.m a triplet of relative intensity 1H is observed and is assigned to the CH proton coupling with CH_3 protons, $^4J(C\underline{H}\text{-}C\text{-}C\underline{H}_3) = 2.1$ Hz. A singlet of relative intensity 1H at $\delta = 5.89$ p.p.m. is observed and is assigned to the (–N-N=C-CH) proton. A strong single is observed at $\delta = 2.52$ p.p.m. of relative intensity 3H, assigned to CH_3 protons. Two singlets are observed at $\delta = 1.35$ p.p.m. and $\delta = 2.13$ p.p.m. of relative intensity 3H each, assigned to two methyl protons CH_3 and CH_3. It is difficult to distinguish between the two, shows the ^1H n.m.r spectrum. Coupling to phosphorus by the CH^1 proton is obtained, the signal being a triplet of triplets, $^3J(\underline{P}C\underline{H}) = 12$ Hz; (c) the infrared spectrum was characteristic of a cis-chelated dichloride complex. The υ(N-H) band at 3320 of the starting material was absent.

3.2 Optical properties

The transmittance and reflectance spectra of the $[Ni(Cl)_2\{(Ph_2P)_2CHC(R_1R_2)NHNH_2\}]$ complex crystals were measured over the temperature range 77 to 300 K. The spectra were obtained over the incident photon energy range of 1.29 to 3.93 eV. In Figures 3a and 3b, typical spectra of the transmittance and reflectance for the crystals are shown. These figures show that there is a shift in either the transmittance curves or the reflectance curves toward the lower values of the incident photon energy as the temperature is increased.

It is known that optical measurements are the suitable tools for understanding the band structure, energy gap width and optical parameters of both crystalline and amorphous non-metallic materials. The optical absorption coefficient (α) is related to the transmittance (T) of a sample with thickness (d) through the relation:

$$\alpha = \frac{1}{d}\mathrm{Ln}\left(\frac{1}{T}\right). \quad (1)$$

This relation was used for calculating the values of the absorption coefficient (see Fig. 3c). It is obvious from this figure that the absorption coefficient exhibits a short band tail at low energies. This week absorption tail most probably originates from defects and impurity states within the band gap. Tailing of the band states into the gap may be induced by a large concentration of free carriers, which result a screened Coulomb interaction between carriers that

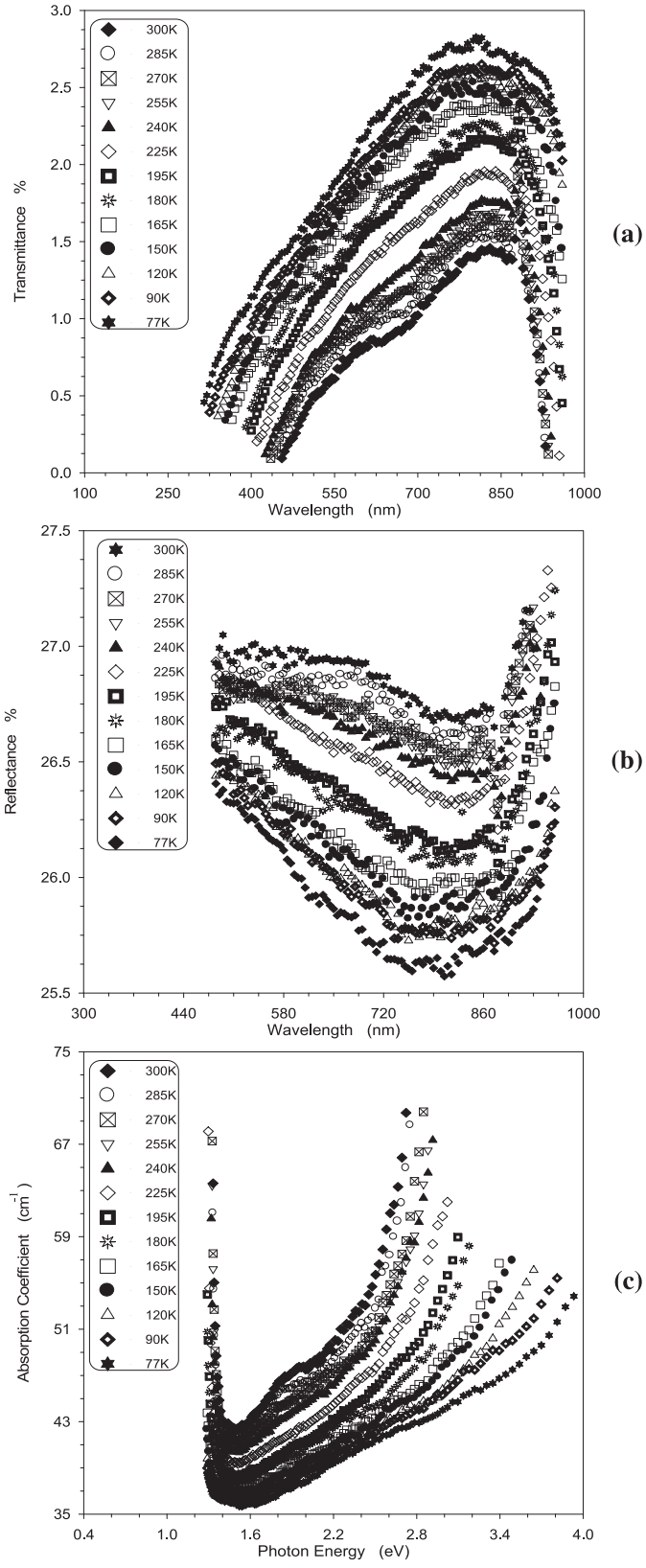

Fig. 3. (a) Temperature dependence of transmittance spectra in the organic crystal "5a", (b) Temperature dependence of reflectance spectra in the organic crystal "5a", (c) Dependence of the absorption coefficient of the organic crystal "5a".

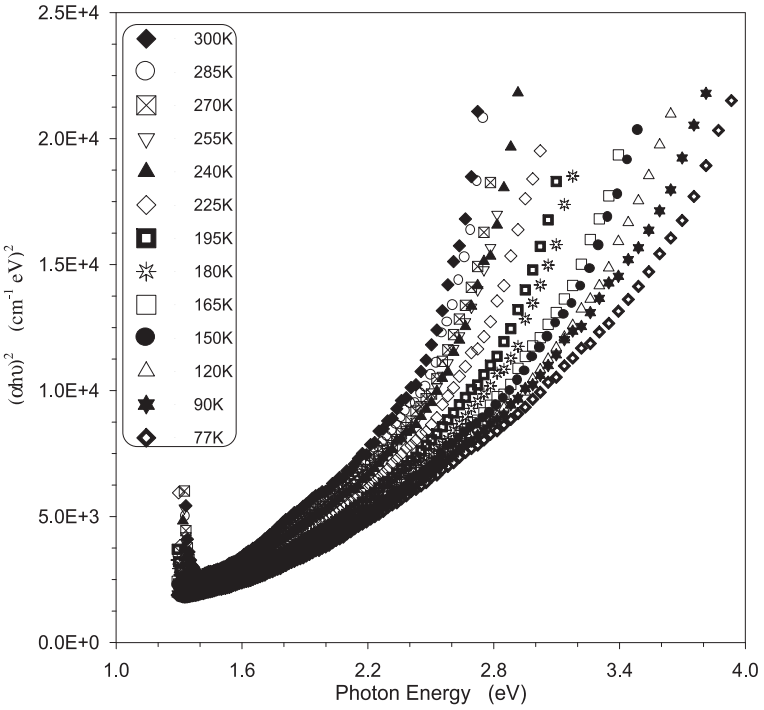

Fig. 4. Shows a plot of $(\alpha h\upsilon)^2$ versus $h\upsilon$.

perturbs the band edges. Thereafter it increases steeply with increasing the photon energy near the fundamental edge. In the region of the photon energy that has values greater than those of the exponential edge region, the absorption coefficient increases linearly with the increasing incident photon energy. These distinct regions are obvious in Figure 5. Also it is clear from this figure that values of the absorption coefficient up to those of the exponential edge region (high absorption region or linear portion) undergo a shift toward low values of the photon energy with increasing temperature.

In the high absorption regions (linear increase of α with increasing the incident photon energy), the fundamental absorption edge is determined by interband absorption theory, in which the relationship between the absorption coefficient (α) and the incident photon energy ($h\upsilon$) is governed by the relation [16,17]:

$$\alpha = \frac{\lfloor A\,(h\upsilon - E_g)^n \rfloor}{h\upsilon}, \tag{2}$$

where, A is an energy-independent constant depending on the transition probability, E_g is the width of the band gap, and n is an index that characterizes the optical absorption processes in $[Ni(Cl)_2\{(Ph_2P)_2CHC(R_1R_2)NHNH_2\}]$ complex crystals. The analysis of the experimental results showed that a proportionality is revealed between the absorption coefficient and the frequency of the photon energy as $(h\upsilon - E_g)^n$. The exponent n can take one of the four values: 2, 1/2, 3 and 3/2, which define the type of the optical transition. Theoretically n is equal to 2, 1/2, 3 or 3/2 for the indirect allowed, direct allowed, indirect forbidden and direct forbidden transitions, respectively [18]. The case of the organic crystals under investigation, the exponent n indicates that the dominant transition is a direct allowed one. Therefore, $(\alpha h\upsilon)^2$ was plotted against $(h\upsilon)$ and this graph is described in Figure 4. On other hand, the usual method for determining the type of the optical transition includes plots of $(\alpha h\upsilon)^{1/n}$ versus the incident photon energy $(h\upsilon)$. This requires a set of plots with four values of the exponent n: $(\alpha h\upsilon)^{1/2}$, $(\alpha h\upsilon)^2$, $(\alpha h\upsilon)^{1/3}$, and $(\alpha h\upsilon)^{2/3}$. For the plot that satisfies the widest linearity of data, its exponent determines the type of the optical transition. In this work, the optical band gaps were calculated by linear fitting the high absorption regions (the optical band gaps were determined from the straight line of $(\alpha h\upsilon)^2 = f(h\upsilon)$ to $h\upsilon = 0$). These fits intersect the $h\upsilon$-axis at the values of the optical band gap widths of the $[Ni(Cl)_2\{(Ph_2P)_2CHC(R_1R_2)NHNH_2\}]$ crystals at the values of temperature under investigation. The figure also suggests that above the absorption edge, there is a horizontal shift toward low photon energy as the temperature increases (the increase in the motion of the atoms broadens the energy levels). Where; as the temperature increases, the lattice expands and the oscillations of the atoms around their equilibrium lattice points increase. There is also an electron-lattice interaction, which depends strongly on temperature: at temperatures much lower than the Debye temperature, the gap width varies proportionally with the square of the temperature, whereas much above the Debye temperature the gap width varies linearly with the temperature [14]. The temperature dependence of the band gap with for many semiconductors is usually fitted by the following empirical relation [7]:

$$E_g(T) = E_g(0) - \left(\frac{\alpha T^2}{T+\beta}\right) \tag{3}$$

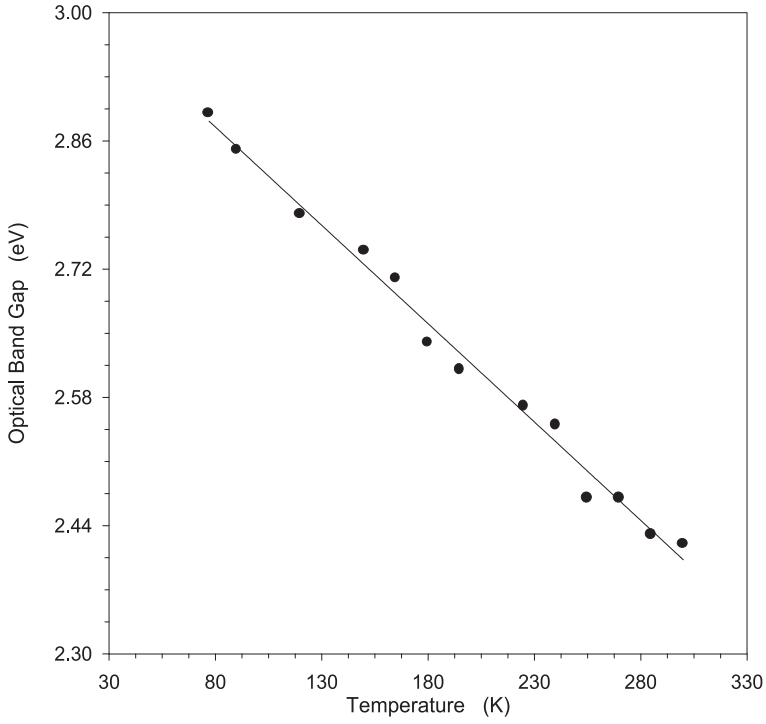

Fig. 5. Shows the temperature dependence of the optical band gap.

where, $E_g(0)$ is the value of the energy gap at 0 K; and α and β are constants. The temperature dependence of the optical band gap over the investigated range of temperature is depicted in Figure 5. Using equation (3) and Figure 5, both α and β were estimated and found to be 2.11×10^{-3} and 6.442, respectively. The temperature coefficient of the optical gap width may also be calculated from the linear portion of Figure 5 (high region of the temperature range under investigation). The temperature coefficient of the optical gap width (dE_g/dT) was calculated to be -2.14×10^{-3} eV/K. It is well-known that the charge transport properties of organic semiconductors depend on their chemical structure [19]. This is evidence that the organic crystals under investigation show typical semiconductor behavior as a result of the delocalization of the π-electrons in the structure. The electrical conductivity of these crystals was measured and found to be in the semiconducting range. The studied compound possesses many π-electrons extending along the structure, its electron states are delocalized, allowing charge transport.

The refractive indices (n) for the range of temperature investigated can be determined using the following relation. The reflection coefficient affecting the intensity of the radiation is given by the following relation for normal irradiance:

$$R = \frac{(n-1)^2 + k^2}{(n+1)^2 + k^2}. \tag{4}$$

However, the $[Ni(Cl)_2\{(Ph_2P)_2CHC(R_1R_2)NHNH_2\}]$ complex crystals are transparent. Therefore, the above relation can be rewritten for the transparent range of irradiance in the form:

$$R = \left(\frac{(n-1)}{(n+1)}\right)^2. \tag{5}$$

The refractive index as a function of incident photon energy (1.29 to 2.55 eV) is plotted in Figure 6a over the investigated range of temperature. It is evident from this figure that: below the absorption edge and in the low photon energy region (1.63 to 1.86 eV), the dispersion of the refractive index is normal over the whole investigated range of temperature and can be described well using a single oscillator model [20]. The dispersion plays important role in the research of optical materials due to a significant role in optical communications and in designing devices for spectral dispersion. Below the absorption edge, dispersion of the refractive index is governed by the relation:

$$n^2 = 1 + \frac{E_o E_d}{E_o^2 - (h\upsilon)^2} \tag{6}$$

$$\Rightarrow (n^2-1)^{-1} = \frac{E_o}{E_d} - \left(\frac{1}{E_o E_d}\right)(h\upsilon)^2 \tag{7}$$

where, E_o is the average excitation energy for electronic transitions (the single oscillator energy); E_d is a measure for the strength of the interband optical transitions (the dispersion energy); and ($h\upsilon$) is the incident photon energy. It is observed from Figure 6a that in the mentioned low photon energy region, the refractive indices over the whole studied temperature range vary linearly with the incident photon energy. Both the single oscillator energy (E_o) and the dispersion energy (E_d) can be obtained for all investigated temperatures by plotting $(n^2-1)^{-1}$ as a function of the photon energy $(h\upsilon)^2$ in the photon energy range: (1.29 to 2.55 eV). A linear portion of this plot is observed in the photon energy region 1.63 to 1.86 eV (see the inset of Fig. 6b). The E_d and E_o were calculated from the slope $(E_oE_d)^{-1}$ and the intercept (E_o/E_d), which is depicted in Figure 6b.

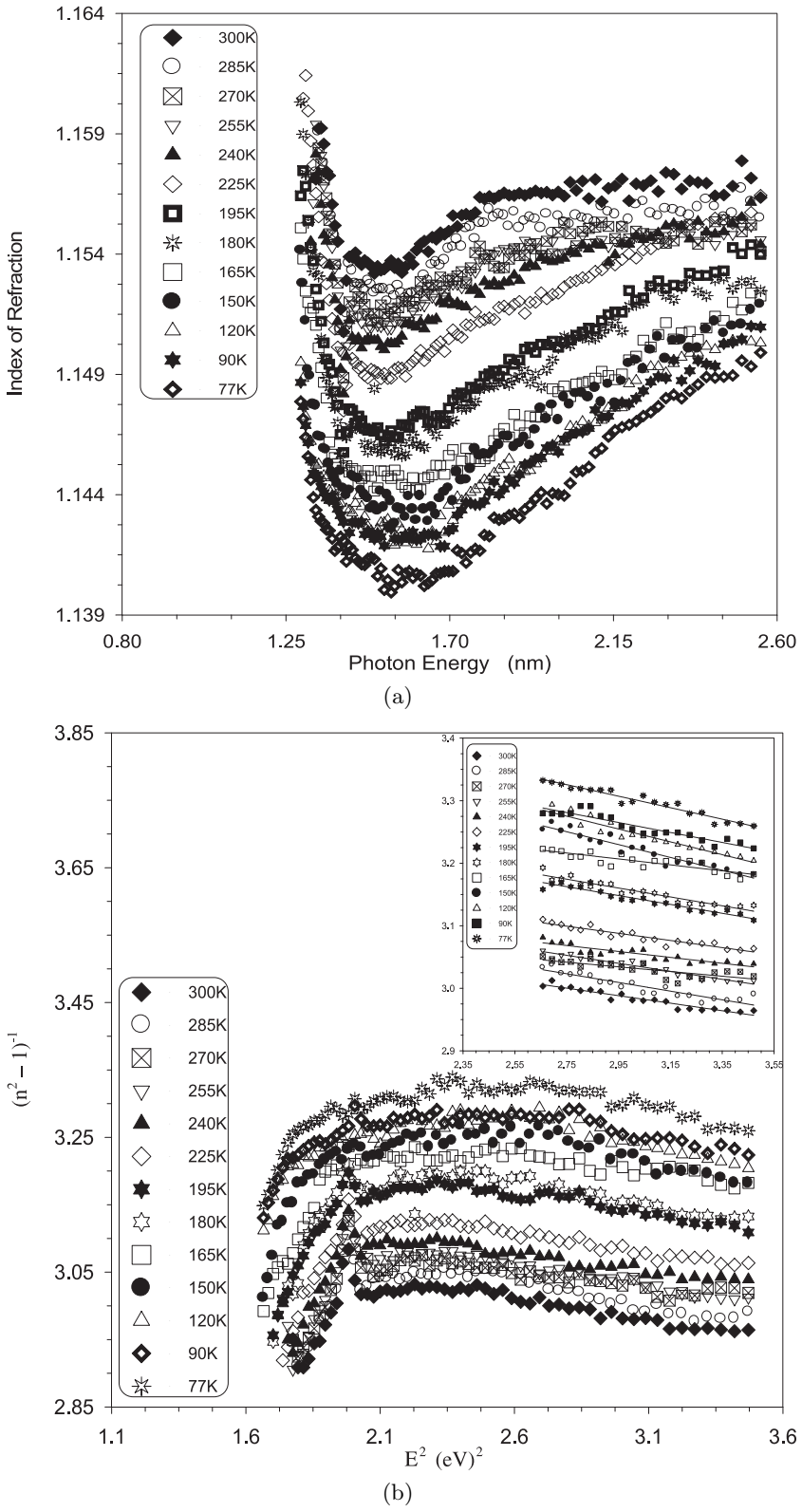

Fig. 6. (a) Shows the dependence of the refractive index (n) on the incident photon energy, (b) Shows the plot of $(n^2-1)^{-1}$ versus $(h\upsilon)^2$.

Table 3. Optical characterization of the organic crystals under investigation.

Temperature (K)	Optical band width (eV)	Oscillator energy (eV)	Dispersion energy (eV)
77	2.89	6.24	1.743
90	2.85	6.632	1.895
120	2.78	5.889	1.655
150	2.74	5.868	1.661
165	2.71	8.397	2.509
180	2.64	6.893	2.046
195	2.61	6.877	2.048
225	2.57	7.551	2.318
240	2.55	8.222	2.57
255	2.47	7.108	2.202
270	2.47	9.172	2.916
285	2.43	6.81	2.117
285	2.43	6.81	2.117
300	2.42	7.25	2.291

The calculated values of the oscillator energies (E_o), the dispersion energies (E_d), and the optical band widths (E_g) for the $[Ni(Cl)_2\{(Ph_2P)_2CHC(R_1R_2)NHNH_2\}]$ complex crystals in the temperature range 77 to 300 K are summarized in Table 3. The static refractive index ($n(0) = (1 + E_d/E_o)^{1/2}$) and the static dielectric constant ($\varepsilon_s = n^2(0)$) were calculated using the above reported relation and found to be 1.053 and 1.109, respectively. Table 3 includes the calculated values of optical gap width, oscillation and dispersion of the refractive index for the organic crystals under study in the investigated temperature range 77 to 300 K.

4 Conclusion

The synthesis of an apyrazole derivative of the diphenylphosphino-methane hydrazine complexes $[Ni(Cl)_2\{(Ph_2P)_2CHC(R_1R_2)NHNH_2\}]$ was reported and the temperature dependences of the optical properties were also studied. The transmittance and reflectance spectra of the crystals were measured over the temperature range 77 to 300 K. The recorded spectra were carried out over the incident photon energy range 1.29 to 3.93 eV. It was found that there is a shift in either the transmittance curves or reflectance curves toward lower values of the incident photon energy with increasing temperature. The absorption coefficient also exhibits a short band tail at low energies, which most probably originates from defects and impurity states within the band gap. Tailing of the band states into the gap may be induced by a large concentration of free carriers, which result in a screened Coulomb interaction between carriers that perturbs the band edges. In line with the calculated optical parameters, the compound under investigation is a typical organic semiconductor. The type of the optical transition was determined in the organic crystals under study to be direct allowed one. The direct allowed gap and its temperature coefficient are also determined to be $\sim$2.42 eV and $\sim -2.14 \times 10^{-3}$ eV/K, respectively. Finally, the temperature dependence of refractive index was investigated. As a result of this investigation, all of the oscillator E_o and the dispersion E_d energies of the refractive index, the static refractive index and the static dielectric constant were calculated over the investigated range of temperature.

References

1. R.V. Rao, M.H. Shridhar, S. Ganesh, K.C. Prashanth, Chem. Phys. Lett. **341**, 306 (2001)
2. M.R. Baldo et al., Nature (London) **403** 750 (2000)
3. S.R. Forrest, Nature (London) **428**, (2004) 911; T.W. Kelley, P.F. Baude, C. Gerlach, D.E. Ender, D. Muyres, M.A. Haase, D.E. Vogel, S.D. Theiss, Chem. Mater. **16**, 4413 (2004)
4. C.D. Dimitrakopoulos, P.R.L. Malenfant, Adv. Mater. (Weinheim Ger) **14**, 99 (2002)
5. F.A. Hegmann, R.R. Tykwinski, K.P.H. Lui, J.E. Bullock, J.E. Anthony, Phys. Rev. Lett. **89**, 227403-1 (2002)
6. A. Toza, P.C. Vinodkumar, R.G. Patel, PRAMANA - J. Phys. **60**, 535 (2003)
7. J.I. Pankove, *Optical process in semiconductors* (Prentice Hall Inc., 1971), p. 45
8. F. Urbach, Phys. Rev. **92**, 1324 (1953)
9. M.H. Araujo, P.B. Hitchcock, J.F. Nixon, M.D. Vargas, J. Braz. Chem. Soc. **9**, 563 (1998)
10. P. Braunstein, J.R. Galsworthy, B.J. Hendan, H.C. Marsmann, J. Organomet. Chem. **551**, 125 (1998)
11. P. Braunstein, Actual. Chim. **7**, 75 (1996)
12. N. Nawar, A.K. Smith, Inorg. Chim. Acta **227**, 79 (1994)
13. N. Nawar, J. Chem. Res. (s) 498 (1994)
14. M.M. Harding, B.S. Nicholls, A.K. Smith, Acta Crystallogr. Sect. C **40**, 790 (1984)
15. D.F. Foster, J. Harrison, B.S. Nicholls, A.K. Smith, J. Organomet. Chem. **295**, 99 (1985)
16. J.I. Pankove, "*Optical processes in Semiconductors*" (Prentice-Hall, New Jersey, 1971), p. 93
17. J. Tauc, "*Amorphous and Liquid Semiconductors*" (Plenum, New York, 1974), Chap. 4
18. A.F. Qasrawi, Cryst. Res. Technol. **40**, 610 (2005)
19. J.P. Farges, *Organic conductors* (N.Y., 1994)
20. C. Baban, G.I. Rusu, P. Prepelita, J. Optoelectronics and Advanced Materials, **7** 817 (2005)